

Bull Yamaguchi Med Sch 62(1-2):11-19, 2015

Added Value of MR Myelography Using a Fat-Suppressed-Three Dimensional Coherent Oscillatory State Acquisition for the Manipulation of the Image Contrast Sequence in the Diagnosis of Lumbar Canal Stenosis: Comparison with Routine MR imaging

Takaaki Ueda¹, Osamu Tokuda², Yuko Harada¹, Etsushi Iida¹, Kenzo Shirasawa³, Akihisa Yamashita³, Bungo Hosoda⁴, Naofumi Matsunaga¹

¹ Department of Radiology, Yamaguchi University Graduate School of Medicine, 1-1-1 Minami-kogushi, Ube, Yamaguchi 755-8505, Japan

² Department of Radiology, Kanmon Medical Center, Yamaguchi, 1-1 Cyofu-sotourachou, Shimonoseki, Yamaguchi 752-8510 Japan

³ Department of Orthopedics Surgery, Shimonoseki City Central Hospital, 1-13-1 Kouyouchou Shimonoseki, Yamaguchi, Japan

⁴ Division of Radiological Technology, Shimonoseki City Central Hospital, 1-13-1 Kouyouchou Shimonoseki, Yamaguchi, Japan

(Received December 11, 2014, accepted January 29, 2015)

Correspondence to Takaaki Ueda, MD E-mail: t.ueda@yamaguchi-u.ac.jp

Abstract Objective: To evaluate whether 3D magnetic resonance myelography (MR myelography) using fat-suppressed-three dimensional coherent oscillatory state acquisition for the manipulation of the image contrast (FS 3D-COSMIC) sequence has additional diagnostic value in the diagnosis of lumbar canal stenosis.

Materials and Methods: The patient population consisted of 30 patients who were seen for the diagnosis of lumbar canal stenosis. The lumbar segments were divided into 15 groups, from L1-L2 to L5-S1; right, middle and left. Of all segments examined (450 segments), 180 segments confirmed to have stenosis by surgery were included in this study. The sensitivities, specificities, and accuracies of observer for diagnosing lumbar canal stenosis of the routine MRI + MR myelography were compared with those of the routine MRI alone. In addition, receiver operating characteristic analysis was performed.

Results: In all segments, both the sensitivity, accuracy and Az value were significantly higher for the routine MRI + MR myelography than for the routine MRI alone ($P < 0.05$).

Conclusion: The addition of MR myelography using the FS 3D-COSMIC sequence to routine MR imaging may be useful for evaluating lumbar canal stenosis; especially, the technique may contribute to improving the sensitivity for the diagnosis of lumbar canal stenosis.

Key words: MRI, COSMIC, myelography, canal stenosis

Introduction

Both myelography and computed tomography (CT)-myelography are useful for surveying the dural sac and nerve root. However, these examinations have disadvantages, such as their invasive nature and the radiation exposure¹. In contrast, magnetic resonance (MR) myelography is based on a heavily T2-weighted imaging technique and produces a high signal from cerebrospinal fluid. This imaging sequence, which was first described in 1992, produces an effect which gives images similar to conventional myelography². Some investigators have shown the usefulness of MR myelography in patients with lower back pain³⁻⁶. MR myelography can also produce myelogram-like images without the use of contrast agent. Scarabino et al. (1996) demonstrated the usefulness of MR myelography in comparison with conventional MR in 21 patients with lower back pain⁷. Hofman and Wilmin (1996) described the use of MR radiculopathy to increase the sensitivity of conventional magnetic resonance imaging (MRI) in the diagnosis of nerve root compression in 19 patients, but did not discuss the imaging or clinical correlation⁸. However, MR myelography has not been adequately scientifically validated regarding whether it can enhance the diagnostic accuracy of MRI.

Previously, MR myelography images were obtained using 2D -fat- suppressed coronal T2-weighted Fast Spin Echo (FSE) images which were reconstructed as maximum intensity projections^{2,5}. Recently, some investigators have described the usefulness of 3D-MR myelography for evaluating the brachial plexus and lumbosacral plexus; these included the 3D -short inversion-time inversion recovery (STIR) single slab with variable flip angle distribution (SPACE) sequence, 3D -heavily T2-weighted MR myelography sequences and, the diffusion-weighted (DW) neurography sequence with fiber tracking reconstruction (tractography)^{9,10}.

The fat-suppressed three-dimensional coherent oscillatory state acquisition for the manipulation of image contrast (FS 3D-COSMIC) is a sequence that is based on fast imaging employing steady state acquisition (FIESTA) of balanced steady-state free

precession (balanced SSFP). Amakawa et al. (2010) reported that the FS 3D-COSMIC technique could improve the contrast of the cartilage and synovial fluid with high spatial resolution¹¹. However, no investigators have evaluated the FS 3D-COSMIC technique for the use in MR myelography sequences.

The objective of the current study was to evaluate the additional advantage of using MR myelography in patients who underwent both lumbar spine MRI and surgery in the diagnosis of lumbar canal stenosis.

Materials and Methods

Patients

The current study included 30 patients suspected of having lumbar disease. The patients underwent both routine MRI scans, combined with magnetic resonance (MR) myelography and surgery during the period from April 2010 to January 2011. Fifteen females and 15 males diagnosed with lumbar stenosis by an experienced orthopedic surgeon were included in the current study. All patients underwent surgery. The age of the patients ranged from 17 to 93 years and the mean age was 65.1 ± 19.3 years. The institutional review board gave its approval, and informed consent was obtained from all subjects included in this study.

MR imaging technique

All examinations in the 30 patients were performed using a 1.5 T whole body MR system (Signa Horizon, GE Medical Systems, Milwaukee, WI) using a spine array coil. First, the routine protocol was initially performed as follows: Sagittal T1-weighted FSE images were obtained using the following parameters: TR/TE = 550/14 ms; echo-train length (ETL) = 5; slice thickness = 4 mm, gap = 0.4 mm; FOV = 16 cm, matrix = 320×224 ; number of excitations = 3 and a total acquisition time = 1 minute, 46 seconds. Sagittal T2-weighted FSE imaging was performed using the following parameters: TR/TE = 2700/110 ms; ETL = 16; slice thickness = 4 mm; gap = 0.4 mm; field of view (FOV) = 16 cm; matrix = 384×256 ; number of excitations = 3; bandwidth = ± 32 kHz; and a total acquisition time = 2 minutes, 11 seconds. Transverse

T1-weighted FSE imaging was performed using the following parameters: TR/TE = 650/14 ms; ETL = 5; slice thickness = 4 mm; gap = 2 mm; FOV = 16 cm; matrix = 256 × 224; number of excitations = 2; bandwidth = ± 22.7 kHz; and a total acquisition time = 2 minutes 6 seconds. Transverse T2-weighted FSE imaging was performed using the following parameters: TR/TE = 3100/110 ms; flip angle = 90°; slice thickness = 4 mm; gap = 2 mm; FOV = 16 cm; matrix = 256 × 192; number of excitations = 16; bandwidth = ± 25 kHz and a total acquisition time = 1 minute, 58 seconds. Additional MR myelography was performed as follows: FS 3D-COSMIC images were obtained using the following parameters: TR/TE = 5.5/2.7 ms; flip angle = 45°; FOV = 300mm; matrix = 320 × 224; bandwidth = 62.5kHz per pixel and an acquisition time = 3 minutes 40 seconds. Both oblique images were obtained by rotating the coronal view image using a software program (Virtual Place, AZE Inc., Tokyo, Japan). Oblique MPR images were obtained by parallel to neural foramina. Maximum intensity projection (MIP) reconstruction was not applied to make oblique reconstructions from the coronal sequences.

Image analysis

Two musculoskeletal radiologists (O.T.; 21 years of experience, Y.H; 10 years of experience) who were blinded to the result of the spinal surgery and the original radiology reports independently evaluated the two sets of MR images retrospectively. The readers first evaluated the routine MR images alone, and at a second session two weeks later, they evaluated both routine MR images and MR myelography images. The images obtained for each patient were randomly presented at each reading session and were evaluated using a 3D-DICOM viewer (Virtual Place, AZE Inc., Tokyo, Japan). MR myelography images were evaluated by original and oblique images. The lumbar segments were divided into 15 groups, from L1-L2 to L5-S1; right, middle, and left. The lateral nerve root portion was defined as a tubular-shaped region in which the nerve root passes from the thecal sac to the intervertebral foramen¹². The middle portion was defined as the part between the right and left thecal sacs. A four-point scale was used to grade each lesion: grade 0 = normal, grade 1 = probable absence of stenosis (Figure 1), grade 2 = probable presence of stenosis (Figure 2) and grade 3 =

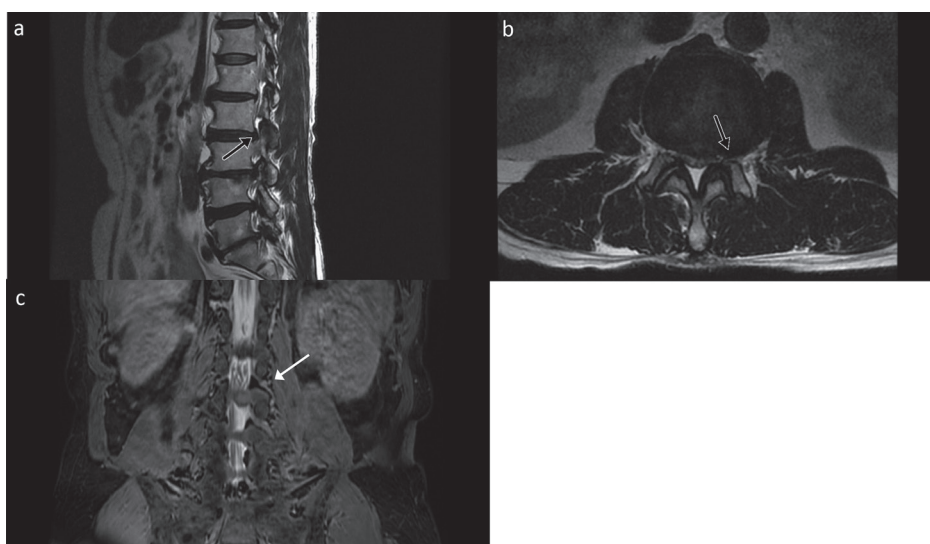


Figure1. (Grade 1)

A 60-year-old male who had acute lower back pain.

Sagittal (a) and axial (b) T2-weighted images showed a disc herniation (black arrow) on the left side at L2-3.

(c) Magnetic resonance myelography demonstrated slight compression on the left side thecal sac at the L2 nerve root (white arrow). The lesion of the left portion at L2-3 was rated as grade 1 by both readers.

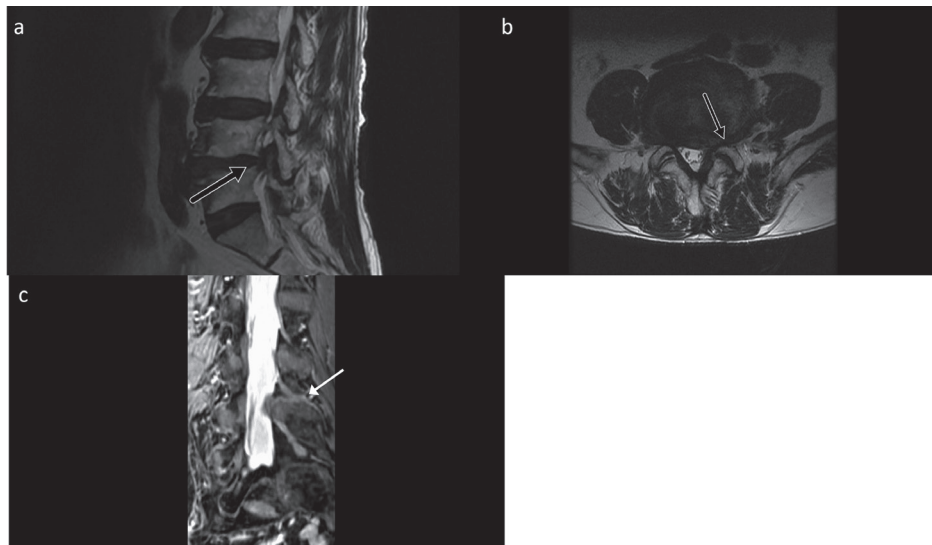


Figure 2. (Grade 2)

A 78-year-old male who presented with a two week history of left leg pain.

Sagittal (a) and (b) axial T2-weighted images showed a disc herniation (black arrow) on the left side at L4-5.

(c) Magnetic resonance myelography showed L4 nerve root running transversely, and demonstrated mild compression of the left side thecal sac at the L4 nerve root (white arrow). The lesion of left portion at L4-5 was rated as grade 2 in both readers.

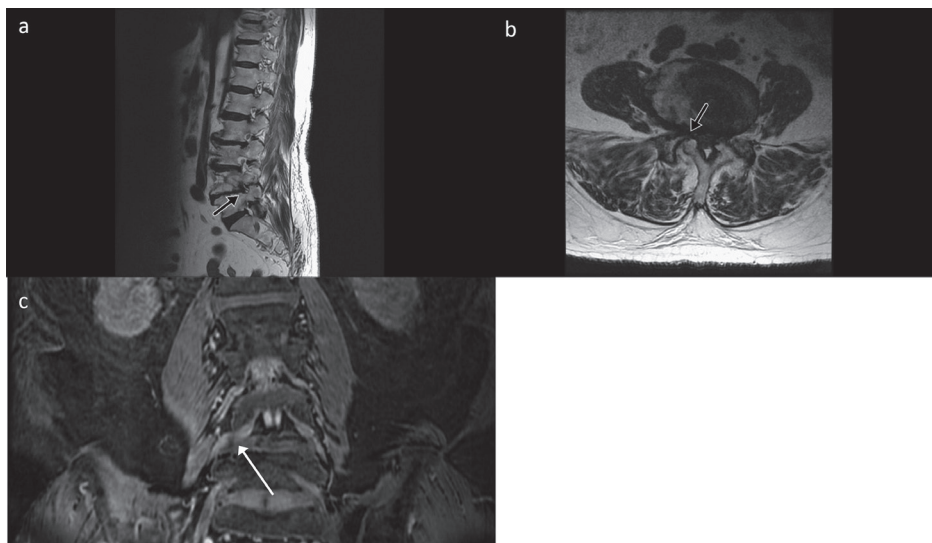


Figure 3. (Grade 3)

An 84-year-old female presented with a one-month history of right leg pain.

Sagittal (a) and axial (b) T2-weighted images showed a disc herniation (black arrow) on the right side at L4-5.

(c) Magnetic resonance myelography demonstrated severe compression of the right side thecal sac and obstruction of the dorsal root ganglions at the L4 nerve root (white arrow). The lesion in the right portion at L4-5 was rated as grade 3 by both readers.

definite presence of stenosis (Figure 3).

Gold standard

Surgical operations were performed by two experienced orthopedic surgeons (K.S. with 30 years of experience in spinal surgery, A.Y. with 15 years of experience in spinal surgery). Of the 180 segments examined by surgery, 65 lumbar segments (L1-2 level, n = 2; L2-3 level, n = 3; L3-4 level, n = 14; L4-5 level, n = 30; L5-S level, n=16) in which canal stenosis were found during the surgery were included in the current study (Table 1). The surgical methods performed in our study include decompressive laminectomy and posterolateral fusion using a local bone graft with or without instrumentation. The interval between preoperative MRI and surgery varied from 1-90 days, the mean \pm SD was 18.0 \pm 19.9 days.

Statistical analysis

In all segments, the sensitivities, specificities and accuracies of both routine MRI alone and routine MRI + MR myelography using the FS 3D-COSMIC sequence were calculated for both readers in the central (intra-spinal canal), lateral (intra-foraminal), and whole segments at each intervertebral level. The ratings of the images in the diagnostic performance were used to calculate the sensitivities, specificities, and accuracies of each reader for diagnosing lumbar canal stenosis or lumbar disc herniation. Ratings of 0-1 indicated a reading of an absence of the segments, and ratings of 2-3 indicated the presence of the segments. Second, the sensitivities, specificities, and accuracies of the routine MRI + MR myelography were compared with those of the routine MRI alone by using paired t-tests. Third, the weighted

κ values (w-k) were calculated to assess inter-reader variability in the assignment of the ratings. The level of agreement was defined as follows: w-k < 0.00 indicated no agreement; a w-k = 0.00-0.40 indicated a poor agreement; a w-k of 0.41-0.75 represented a good agreement; and a w-k of 0.76-1.00 represented an excellent agreement. The *P* values < 0.05 were considered to indicate a statistically significant difference.

Finally, the receiver operating characteristic (ROC) curves were calculated to compare the diagnostic accuracy of routine MRI + MR myelography with that of routine MRI in 65 segments which had confirmed final diagnoses made during the surgical procedures. The diagnostic capability was determined by calculating the area under each reader-specific ROC curve (*Az*). The results were expressed as the mean *Az* \pm standard deviation (SD). The *Az* values for the routine MRI + MR myelography were compared with those for the routine MRI using the paired *t*-test for both readers. All statistical analyses were performed by using a special software program (SPSS, release 18.0 for windows, Chicago, IL).

Results

The results of the diagnostic performance of routine MRI alone and routine MRI + MR myelography in 180 segments of 30 patients for both readers are listed in Tables 2 and 3. In the lateral segment, both the sensitivity (93.8% vs.71.9%) and accuracy (94.2% vs.85%) were significantly higher for routine MRI + MR myelography than those for routine MRI alone for reader 1 (sensitivity, *P* < 0.05; specificity, *P* < 0.05). Both the sensitivity (87.5% vs. 65.6%) and accuracy (93.3% vs. 82.5%) were also significantly higher for the routine

Table 1 Numbers of Lesions in Surgical Findings

		Right	Midle	Left
Results of Surgical Findings (n = 65)	L1-2	0	2	0
	L2-3	1	2	0
	L3-4	3	7	4
	L4-5	8	15	7
	L5-S	6	7	3
Total		18	33	14

Table 2 Results of Diagnostic Performance in Lumbar Canal Stenosis by Reader 1

		Routine MRI	MRI + MRM	95% CI	<i>P</i> value
Central Portion	Sensitivity	87.8(29/33) ± 33.1	90.9 (30/33) ± 29.2	-18.4 to 12.3	0.69
	Specificity	81.5 (22/27) ± 39.6	85.2 (23/27) ± 36.2	-24.4 to 17.0	0.72
	Accuracy	85 (51/60) ± 36.0	88.3 (53/60) ± 32.3	-15.7 to 9.0	0.59
Lateral Portion	Sensitivity	71.9 (23/32) ± 45.7	93.8 (30/32) ± 24.6	-40.2 to -3.5	<0.05
	Specificity	89.8 (79/88) ± 30.5	94.3 (83/88) ± 23.3	-12.6 to 3.5	0.26
	Accuracy	85 (102/120) ± 35.9	94.2 (113/120) ± 23.5	-16.9 to -1.45	<0.05
All Portions	Sensitivity	80 (52/65) ± 40.3	92.3 (60/65) ± 26.8	-24.2 to -0.04	<0.05
	Specificity	87.8 (101/115) ± 32.8	92.2 (106/115) ± 26.9	-5.9 to 14.6	0.27
	Accuracy	85(153/180) ± 39.3	92.2 (166/180) ± 26.9	-13.7 to -0.6	< 0.05

Note. - Data are percentages ± standard deviation. Numbers in parentheses are raw data. MRM = MR myelography, CI=confidence interval

Table 3 Results of Diagnostic Performance in Lumbar Canal Stenosis by Reader 2

		Routine MRI	MRI + MRM	95% CI	<i>P</i> value
Central Portion	Sensitivity	72.7(24/33) ± 45.2	81.8 (27/33) ± 39.2	-29.8 to -11.7	0.38
	Specificity	88.9 (24/27) ± 32.0	85.2 (23/27) ± 36.2	-14.9 to 22.3	0.69
	Accuracy	80 (48/60) ± 40.3	83.3 (50/60) ± 37.6	-17.4 to 10.7	0.64
Lateral Portion	Sensitivity	65.6 (21/32) ± 48.2	87.5 (28/32) ± 33.6	-42.6 to -1.1	<0.05
	Specificity	88.6 (78/88) ± 31.9	95.5 (84/88) ± 20.9	-14.9 to 1.2	0.09
	Accuracy	82.5 (99/120) ± 38.1	93.3 (112/120) ± 25.0	-19.0 to -2.6	<0.05
All Portions	Sensitivity	69.2 (45/65) ± 46.5	84.6 (55/65) ± 36.4	-29.8 to -0.8	< 0.01
	Specificity	88.7 (102/115) ± 31.8	93 (107/115) ± 25.6	-14 to 5.5	0.25
	Accuracy	81.7 (147/180) ± 38.8	90.0 (162/180) ± 9.1	-17.8 to -1.1	< 0.01

Note. - Data are percentages ± standard deviation. Numbers in parentheses are raw data. MRM = MR myelography, CI=confidence interval

MRI + MR myelography than for the routine MRI alone for reader 2 (sensitivity, $P < 0.05$; specificity, $P < 0.05$). In all segments, both the sensitivity (92.3% vs. 80.0%) and accuracy (92.2% vs. 85.0%) were significantly higher for routine MRI + MR myelography than for routine MRI alone for reader 1 (sensitivity, $P < 0.05$; specificity, $P < 0.05$). Both the sensitivity (84.6% vs. 69.2%) and accuracy (90.0% vs. 81.7%) were also significantly higher for routine MRI + MR myelography than for routine MRI alone for reader 2 (sensitivity, $P < 0.01$; specificity, $P < 0.01$).

Good agreements were found for routine MRI ($w-k = 0.71$) and routine MRI + MR myelography ($w-k = 0.70$) (Table 4). There were

no absent or poor agreements for the evaluation of inter-reader variability in the comparisons of routine MRI alone and routine MRI + MR myelography.

The Az value for reader 1 was 0.86 ± 0.03 (95% CI: 0.80-0.92) for routine MRI, in contrast, it was 0.92 ± 0.02 (95% CI: 0.87-0.96) for routine MRI + MR myelography (Fig. 4a). The mean Az values for reader 2 were 0.86 ± 0.03 (95% CI: 0.79-0.92) for routine MRI and, 0.90 ± 0.03 (95% CI: 0.85-0.96) for routine MRI + MR myelography (Fig. 4b). The Az value for both readers were significantly higher for the routine MRI + MR myelography than for the routine MRI alone ($P < 0.05$).

Table 4 Intra-Reader Variability for Diagnostic Performance

Weighted kappa value for routine MRI	Weighted kappa value for routine MRI + MRM
0.71 ± 0.05 (0.61, 0.80)	0.70 ± 0.04 (0.61, 0.79)

Note.-numbers in pearenthis are 95%confidence interval. MRM = MR myelograohy. Date are raw date \pm standard deviation.

Figure 4a. Reader1

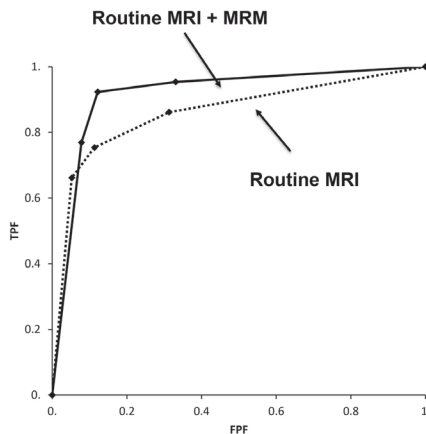
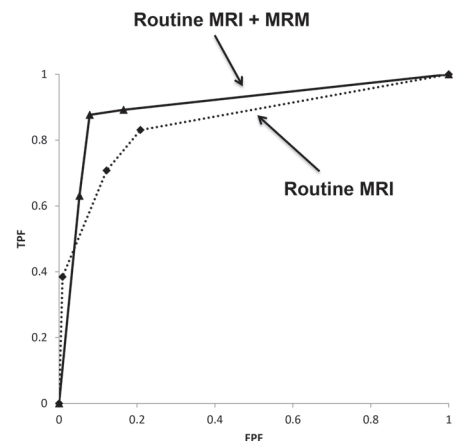


Figure 4b. Reader2



Note. TPF = True Positive Fraction, FPF = False Positive Fraction
MRI = Magnetic Resonance Image, MRM = Magnetic Resonance Myelograph

Figure 4.

(a) The Receiver Operating Characteristic (ROC) curve for routine MRI + MRM (solid line) and routine MRI (dotted line) for reader 1.

The area under the curve for routine MRI + MRM = 0.92 ± 0.02 (95% CI: 0.87-0.96).

The area under curve for routine MRI = 0.86 ± 0.03 (95% CI: 0.80-0.92).

(b) The ROC curve for routine MRI + MRM (solid line) and routine MRI (dotted line) for reader 2. The area under curve for routine MRI + MRM = 0.90 ± 0.03 (95% CI: 0.85-0.96).

The area under curve for routine MRI = 0.86 ± 0.03 (95% CI: 0.79-0.92).

Discussion

The addition of other MR techniques to routine MRI for the evaluation of lumbar canal stenosis can include two sequences; one is diffusion-weighted (DW) MR neurography, and the other is 3D-MR myelography^{12,13}. DW MR imaging (DWI) has recently been introduced as an alternative way to visualize nerves. DW MR neurography is based on the concept of diffusion-weighted whole-body imaging with background body signal suppression (DWIBS), which allows multiple thin-slice DWI data sets to be obtained^{14,15}. However, DW MR neurography requires longer acquisition time than 3D-MR myelog-

raphy, and provides lower spatial resolution. Therefore, DW MR neurography is rarely performed for routine examination. In contrast, 3D-MR myelography requires a moderate acquisition time, and provides higher spatial resolution than DW MR neurography.

The COSMIC technique is a balanced coherent sequence that utilizes segmented multishot centric acquisition to achieve a mixed T2/T1-weighted contrast. Since the data acquisition of the steady-state transition is filled up with the center of the k-space when using the COSMIC technique, improvement in the contrast of the cartilage, which is a low T2/T1 value domain, is expected¹¹. To the best of our knowledge, no investigators has

previously evaluated the potential of using FS 3D-COSMIC technique for MR myelography sequences. However, 3D-MR myelography using a FS 3D-COSMIC technique may be useful for evaluating lumbar canal stenosis, because the technique provides a great contrast between nerve root and fat or bone tissues.

Rankine¹⁶ et al. (1997) reported that routine MRI (T1- and T2-weighted turbo spin-echo sagittal images, and T2-weighted turbo spin-echo axial images) showed a sensitivity of 60% and a specificity of 95% for the diagnosis of lumbar canal stenosis. In the current study, the sensitivities for both readers for the case with lumbar canal stenosis were 80.0% for reader 1 and 69.2% for reader 2. In contrast, the specificities for the readers were 87.8% for reader 1 and were 88.7% for reader 2. These results concur with the results reported by Rankine et al. Based on our results, the sensitivities in all segments were significantly higher on routine MRI + MR myelography than those on routine MRI alone for both readers. These findings suggest that the main advantage of the additional MR myelography may be an improvement of the sensitivity for the evaluation of lumbar canal stenosis.

In the current study, the sensitivities for the lateral segment were significantly higher on routine MRI alone than were those on routine MRI + MR myelography for both readers. However, there were no significant differences between the sensitivity for routine MRI alone and routine MRI + MR myelography for both readers in the central segment. In central lesions, transverse and sagittal images on routine MRI are helpful for defining the focal nature of a disc protrusion¹⁷. In contrast, our results may show the usefulness of the addition of 3D-MR myelography to routine MR imaging of lateral segments.

Between two radiologists, there are good inter-reader agreement in the weighted kappa values.

The weighted kappa values of routine MRI + MR myelography and routine MRI indicated good agreement (0.70-0.71) among readers. With regard to the inter-reader variability for the diagnostic performance regarding of

lumbar canal stenosis, the weighted kappa value of routine MRI + MR myelography tended to equivalent for that of routine MRI; this result is consistent with that of Song et al¹⁸. In addition, vertebral spurs, thickening of the posterior longitudinal ligament, the flaval ligament and the facet joint might affect the evaluation of the lumbar canal stenosis⁶.

The current study has several limitations. First, the number of patients for whom the results of surgical findings were available was small (n = 30). A larger number of patients might be necessary to confirm the usefulness of the FS 3D-COSMIC sequence in the diagnosis of lumbar canal stenosis. Second, the current study included fewer lesions in the upper intervertebral levels than in the lower intervertebral levels. Finally, a comparison of other MR myelography techniques with the FS 3D-COSMIC sequence was not included in the current study. However, it was difficult to add a routine examination to other 3D-MR myelography sequences in our hospital.

In conclusion, the addition of MR myelography using the FS 3D-COSMIC sequence to routine MR imaging may be useful for evaluating lumbar canal stenosis. In particular, the addition of MR myelography using the FS 3D-COSMIC sequence to routine MR imaging may contribute to improving the sensitivity for the diagnosis of intra- and extra-foraminal stenosis. Further studies with a larger number of patients, and comparing the FS 3D-COSMIC sequence with other 3D MR myelography techniques are therefore needed.

Conflict of Interest

The authors state no conflict of interest.

References

1. Eberhardt, K. E., Hollenbach, H. P., Tomandl, B. and Huk, W. J. Three-dimensional MR myelography of the lumbar spine: comparative case study to X-ray myelography. *Eur. Radiol.*, **7**: 737-742, 1997.
2. Krudy, A. G. MR myelography using

- heavily T2-weighted fast spin-echo pulse sequences with fat presaturation. *Am. J. Roentgenol.*, **159**: 1315-1320, 1992.
3. Hashimoto, K., Akahori, O., Kitano, K., Nakajima, K., Higashihara, T. and Kumasaka, Y. Magnetic resonance imaging of lumbar disc herniation. Comparison with myelography. *Spine*, **15**: 1166-1169, 1990.
 4. Kuroki, H., Tajima, N., Hirakawa, S., Kubo, S., Tabe, R. and Kakitsubata, Y. Comparative study of MR myelography and conventional myelography in the diagnosis of lumbar spinal diseases. *J. Spinal Disorders*, **11**: 487-492, 1998.
 5. Thornton, M. J., Lee, M. J., Pender, S., McGrath, F. P., Brennan, R. P. and Varghese, J. C. Evaluation of the role of magnetic resonance myelography in lumbar spine imaging. *Eur. Radiol.*, **9**: 924-929, 1999.
 6. Pui, M. H. and Husen, Y. A. Value of magnetic resonance myelography in the diagnosis of disc herniation and spinal stenosis. *Aus. radiol.*, **44**: 281-284 2000.
 7. Scarabino, T., Giannatempo, G. M., Perfetto, F., Popolizio, T. and Salvolini, U. [Magnetic resonance myelography with a fast-spin-echo sequence. *La Radiologia medica*, **91**: 202-206, 1996.
 8. Hofman, P. A. and Wilmsink, J. T. Optimising the image of the intradural nerve root: the value of MR radiculography. *Neuroradiol.*, **38**: 654-657, 1996.
 9. Vargas, M. I., Viallon, M., Nguyen, D., Beaulieu, J. Y., Delavelle, J. and Becker, M. New approaches in imaging of the brachial plexus. *Eur. J. Radiol.*, **74**: 403-410, 2010.
 10. Zhang, Z. W., Song, L. J., Meng, Q. F., Li, Z. P., Luo, B. N., Yang, Y. H. and Pei, Z. High-resolution diffusion-weighted MR imaging of the human lumbosacral plexus and its branches based on a steady-state free precession imaging technique at 3T. *Am J Neuroradiol.*, **29**: 1092-1094, 2008.
 11. Amakawa, T., Shinohe, T., Tominaga, S., Honda, T., Fukumaru, M. and Sasaki, J. Fundamental study of the fat-suppressed three-dimensional coherent oscillatory state acquisition for the manipulation of image contrast (3D-COSMIC) sequence in the knee joint cartilage(in Japanese). *Nihon Hoshasen Gijutsu Gakkai zasshi*, **66**: 1221-1228, 2010.
 12. Filler, A. G., Howe, F. A., Hayes, C. E., Kliot, M., Winn, H. R., Bell, B. A., Griffiths, J. R. and Tsuruda, J. S. Magnetic resonance neurography. *Lancet*, **341**: 659-661, 1993.
 13. Yamashita T, T. T., Horie T, et al. <Feasibility of High Resolution Diffusion-weighted MR Neurography for Spinal Nerves.pdf>. *Proc. Intl. Soc. Magn. Reson. Med.*, **11**, 2004.
 14. Takahara, T., Imai, Y., Yamashita, T., Yasuda, S., Nasu, S. and Van Cauteren, M. Diffusion weighted whole body imaging with background body signal suppression (DWIBS): technical improvement using free breathing, STIR and high resolution 3D display. *Radiation medicine*, **22**: 275-282, 2004.
 15. Eguchi, Y., Ohtori, S., Yamashita, M., Yamauchi, K., Suzuki, M., Orita, S., Kamoda, H., Arai, G., Ishikawa, T., Miyagi, M., Ochiai, N., Kishida, S., Masuda, Y., Ochi, S., Kikawa, T., Takaso, M., Aoki, Y., Toyone, T., Suzuki, T. and Takahashi, K. Clinical applications of diffusion magnetic resonance imaging of the lumbar foraminal nerve root entrapment. *Eur. spine J.*, **19**: 1874-1882, 2010.
 16. Rankine, J. J., Hutchinson, C. E. and Hughes, D. G. MRI of lumbar spondylosis: a comparison of sagittal T2 weighted and three sequence examinations. *Br J Radiol.*, **70**: 1112-1121, 1997.
 17. Byun, W. M., Jang, H. W. and Kim, S. W. Three-dimensional magnetic resonance rendering imaging of lumbosacral radiculography in the diagnosis of symptomatic extraforaminal disc herniation with or without foraminal extension. *Spine*, **37**: 840-844, 2012.
 18. Song, K. S., Jang, E. C., Jung, H. J., Kim, K. W. and Yu, H. Observer variability in the evaluation of multiple lumbar stenosis by routine MR--myelography and MRI. *J Spinal Disorders & Techniques*, **21**: 569-574, 2008.